ACS AuthorChoice

Environmental Science & Technology

Article

pubs.acs.org/est

Induction and Coverage Times for Crude Oil Droplets Spreading on Air Bubbles

Mona Eftekhardadkhah and Gisle Øye*

Ugelstad Laboratory, Department of Chemical Engineering, Norwegian University of Science and Technology (NTNU), N-7491 Trondheim, Norway

Supporting Information

ABSTRACT: The interactions between crude oil droplets and air bubbles were studied by the droplet–bubble micromanipulator technique. Eight crude oils were investigated, and some aspects of the involved mechanisms were discussed. The induction time was measured for air bubbles approaching crude oil droplets in different aqueous phases. Distinct differences were observed in the presence and absence of salts, which showed the importance of long-ranged electrostatic repulsive forces on thin-film stability. The results also suggested that adsorption of dissolved hydrocarbons at air bubble surfaces may increase the potential energy barrier in the thin liquid film. Furthermore, the time needed for crude oil droplets to spread over the air bubble surfaces (referred to as coverage time) was determined for the crude oils. The results showed that the spreading velocity decreased with increasing viscosity of the crude oil. The detailed understanding of this type of interaction is considered to be a precursor for improving the oil removal efficiency during the flotation process.

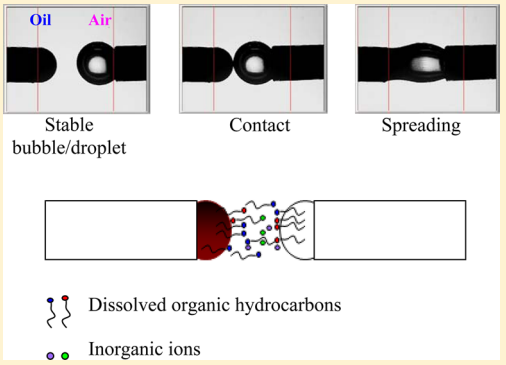

1. INTRODUCTION

Huge quantities of oily produced water are generated during production and processing of crude oil. At the Norwegian continental shelf, the amount of produced water was 116 million m^3 in 2011, while the corresponding amount of crude oil was 97.5 million m^3.[1] The dispersed and dissolved oil present in the water[2] is a source of pollution, and produced water needs to be treated before being discharged to the natural environment. Gas flotation is a well-known method for removing oil droplets from wastewater. The process is based on gravitational separation, where the density difference between the continuous and dispersed phases is increased by the addition of gas to the produced water. This will promote the formation of oil–gas agglomerates.[3,4]

Gas flotation is a complex set of various sub-processes, and optimal oil removal can only be achieved by understanding the controlling mechanisms for each sub-process. To obtain this, it is practical to consider each step separately. The important requirement for successful flotation is quick drainage and rupture of the thin aqueous film that is formed upon close approach between drops and bubbles.[5,6] This will result in oil drops spreading over the gas bubbles, and the oil is removed by flotation. In studies of the thin film between one single drop and one single bubble, the stability is expressed in terms of the induction time, i.e., the time from initial contact of the drop and bubble to rupture of the film.[7,8] Further, it seems accepted that the final rupture of the thin film is due to instabilities in the interfacial regions. This often results in significant variations of the observed induction times.[7,9−15]

The total interactions across the thin film between two approaching drops, two bubbles, or a drop and a bubble are represented by the disjoining pressure and depend upon attractive van der Waals forces and repulsive steric or electrostatic forces. The formation of a stable film requires that the disjoining pressure balance the capillary pressure of the meniscus of the thin liquid film, which forces the liquid out of the film.[7,8] Consequently, it is possible to measure the induction time by recording the dynamic differential pressure across the interfaces.

During the past 20 years, it has been established that interfacial tension, interfacial tension gradients, interfacial shear viscosities, bubble or droplet sizes, and approach velocity are important for the stability of the thin film separating drops or bubbles before coalescence. Furthermore, the presence of surfactants can largely influence the stability of the thin film, because ionic and non-ionic surfactants can introduce potential energy barriers of electrostatic or steric origin.[16] Kumar et al. demonstrated that anionic and cationic surfactants influenced the coalescence time when air bubbles rested at the flat air/water interface.[13] They also studied the binary coalescence of water droplets in different organic phases in the presence of ionic surfactants and absence/presence of inorganic salts.[11] Similar studies were also carried out with non-ionic

Received: August 13, 2013
Revised: October 29, 2013
Accepted: November 25, 2013
Published: November 27, 2013

surfactants.[12] The influence of ionic strength on the binary coalescence of air bubbles in the aqueous surfactant solutions was investigated by Duerr-Auster et al.,[15] while Samanta et al. studied the coalescence of air bubbles at flat interfaces in single-component alcohol and non-ionic surfactant solutions as well as mixed binary alcohol/surfactant solutions.[16] Ata and co-workers pioneered a method for studying binary coalescence of bubbles covered with particles,[9] and more recently, they investigated the binary coalescence of fresh and aged industrial kerosene droplets in water.[7] All of the above investigations involve two-phase systems, while studies of three-phase systems are scarce. The film thinning between an air bubble and oil droplet was reported by Oliveira et al.[6] and was carried out using well-defined model components. To the best of our knowledge, there is only one previous report on the thin-film stability between an air bubble and crude oil droplet.[17]

The objective of this work was to measure the induction time (i.e., the time from first contact to rupture of the thin film separating the droplet and bubble) and the coverage time (i.e., the time required for a crude oil droplet to cover an air bubble) in crude oil−water−air systems. The developed procedures were based on measuring pressure changes across the interfaces upon approaching an oil droplet and air bubble. Eight crude oils and different water compositions were investigated to gain insight into how the chemical composition of the different phases influenced these phenomena. Some mechanistic aspects were also discussed.

2. MATERIALS AND METHODS

2.1. Characterization of Crude Oils. Eight crude oils were used in this study. Extensive characterization of the oils has been reported elsewhere,[18] and they were denoted from A to I. Crude oil D was not included in this study because its high viscosity at room temperature caused blocking of the capillary so that droplets could not be formed.

2.2. Preparation of Brine. Synthetic brine was prepared by dissolving the analytical grade of NaCl (99.5%, Merck, Germany), Na_2SO_4 (99%, Acros, Fair Lawn, NJ), $NaHCO_3$ (99.5%, Merck, Germany), $MgCl_2{\cdot}6H_2O$ (99%, Merck, Germany), and $CaCl_2{\cdot}2H_2O$ (99.5%, Fluka, Czech Republic) in water provided by a Millipore ultrapure water system. The ionic composition of the brine is presented in Table S1 of the Supporting Information. To prevent carbonate precipitation, the brine was stored in a refrigerator and brought to the experimental temperature just before use.

2.3. Drop−Bubble Micromanipulator (DBMM). The measurement of induction and coverage time was performed using a DBMM developed by SINTERFACE, Germany. The DBMM instrument consists essentially of two cells, with each one being a capillary-pressure tensiometer, as illustrated in Figure 1. The paired stainless-steel cells are closed and contain degassed ultrapure water. They also keep the active devices, i.e., the piezo translator and the pressure sensor, in opposite positions. The piezo allows fluid displacements with a full-scale range of ΔV_{pzt} = 188 nL (continuous flux; $\Delta V_{pzt} = 6 \times 10^{-3}$ nL/step) and is used for exact control of the drop/bubble size. Two custom-made metal capillary tubes (0.9 mm outer diameter at the tips) are immersed in an open to the atmosphere optical cuvette (Hellma, 28 × 31 mm^2 inner section) containing the aqueous solution. The capillaries are connected to each of the stainless-steel cells with the horizontally bent tips in conveying directions. Each cell is supported by a metallic frame, which is connected to the other

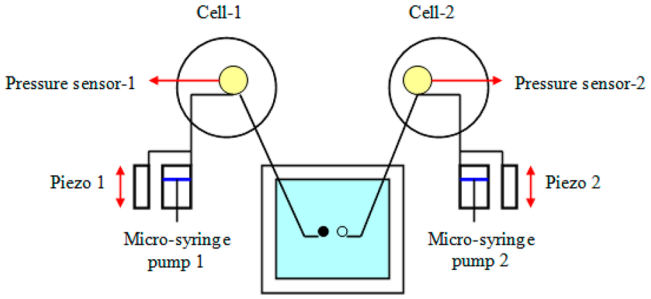

Figure 1. Schematic representation of the DBMM.

frame by an *xyz*-axis micro translation stage, allowing the two capillary tips to face each other at a variable distance. More detailed information can be found elsewhere.[19]

2.4. Methodology for Measuring the Induction Time. Before starting the experiments, the hydrodynamic circuit (including the paired cells and capillaries) was filled with ultrapure degassed water using the lowest speed of the microsyringe pumps under vacuum conditions. This was performed to prevent trapping of air microbubbles in the liquid, something that can cause drop/bubble instabilities. Optical and pressure calibrations were then carried out.[19] The absence of contamination was checked before starting each experiment by creating two water droplets with a similar size in air. The surface tension of these were within 71.96 ± 0.43 mN/m before starting an experiment. Subsequently, sufficient amounts of crude oil and air for creating 10−15 oil drops/bubbles were sucked into the left and right capillaries, respectively.

Initially, an oil drop and air bubble were generated at the tip of the capillaries immersed inside the aqueous solutions. In all of the experiments, the oil drops and air bubbles were 0.45 ± 0.02 and 0.60 ± 0.03 mm in radius, respectively. Coarse and fine adjustment of the drop/bubble size was performed by means of the microsyringe pump and piezo device, respectively.

The radius, area, volume, and differential pressure signal (i.e., pressure difference across the interfaces) were acquired for both drop and bubble as a function of time and distance between drop and bubble. In Figure 2, the time-dependent differential pressures across the oil drop (black dots) and air bubble (light gray dots) interfaces are shown along with the distance between the drop and bubble (dashed line) (see Video a of the Supporting Information). The oil droplet was created first in all experiments. The differential pressure across the oil drop increased during creation of the drop at the tip of the capillary but became constant when the drop reached the predefined size, as illustrated at point a. The same trend was seen for the differential pressure during the formation of the air bubble at the tip of the other capillary. In this case, there was a decrease in the differential pressure before it reached a constant value at b, because the bubble radius was larger than the radius of the capillary. After the drop and bubble were stabilized at the predefined sizes, the air bubble was slowly moved toward the oil droplet. The approach was controlled manually and kept as similar as possible during the experiments. The gap between them reached zero at point c, where the bubble and drop were only separated by a thin aqueous film. The drop in differential pressures, indicated at d, corresponds to rupture of the thin film and the start of crude oil spreading over the air bubble. The induction time reported in this study was the time measured from the time of zero gap to rupture of the thin film, i.e., $t_d - t_c$.

dx.doi.org/10.1021/es403574g | Environ. Sci. Technol. 2013, 47, 14154−14160

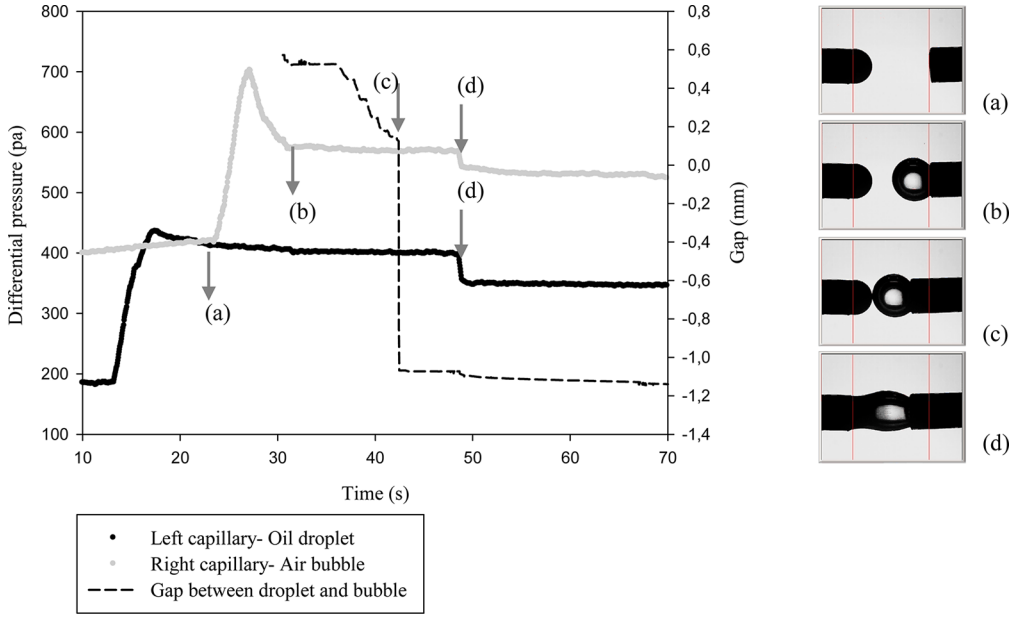

Figure 2. Differential pressure and distance between bubble and drop as a function of time: (a) stable oil drop, (b) stable air bubble, (c) contact (gap = 0), and (d) spreading of crude oil over the air bubble.

In all experiments, the aging time of crude oil droplets ($t_c - t_a$) and air bubbles ($t_c - t_b$) was 25−30 and 10−12 s, respectively. All of the experiments were repeated at a minimum of 10 times for each set of conditions, and the average values and standard deviations are presented (see Table 1).

Table 1. Induction and Coverage Time in Synthetic Brine[a]

crude oil	induction time (s)	coverage time (s)
A	8.00 ± 3.04	0.65 ± 0.15
B	8.75 ± 3.99	2.85 ± 0.91
C	1.01 ± 0.34	5.14 ± 1.16
E	4.11 ± 1.47	1.09 ± 0.33
F	3.28 ± 1.31	1.03 ± 0.38
G	4.79 ± 2.01	5.34 ± 1.20
H	6.34 ± 2.21	1.08 ± 0.54
I	3.84 ± 1.22	2.14 ± 0.95

[a]The values are given as the average and standard deviation of 10 repeated measurements.

3. RESULTS AND DISCUSSION

3.1. Induction Time Measurements. *3.1.1. Influence of Crude Oil Properties.* The induction times when droplets of the different crude oils were approached toward an air bubble are shown in Table 1. The average induction time varied from more than 8 s for crude oil A down to about 1 s for crude oil C. Ata et al. related different induction times prior to coalescence of kerosene drops to the extent and structure of surface-active hydrocarbons accumulated at the drop interfaces.[7] The interfacial properties are important for the range of induction times observed here as well. Crude oils are complex mixtures of hydrocarbons with varying extents of aliphatic and aromatic character. Further, crude oil compounds have various degrees of polarity because of heteroatoms, such as oxygen, nitrogen, and sulfur.[20,21] The most polar components will, even at small amounts, accumulate at the oil−water interface and decrease the interfacial tension. In addition, elastic interfacial layers might build up. Consequently, it is anticipated that accumulation of polar crude oil components at the interface can influence the stability and rupture of the thin film separating a drop and gas bubble, even though the detailed mechanisms are not yet clear.

The repeatability of induction times ranged from about 30 to 45%. This relatively large variation can be attributed to the random nature of the disturbances that caused thinning and breakage of the thin aqueous films. The origin of these disturbances are not still completely understood, but it has been suggested that it can be related to the shapes of the menisci and film surfaces, difference in density of surfactant adsorption layers caused by thermal fluctuations or accidental convections, or corrugations of the film surfaces because of random fluctuation of capillary waves.[22] Different approaching speeds have also been reported to cause variations in this type of measurement.[23] Additional factors that could give rise to variations in film stability are the manual setting of the zero gap, which might lead to variations in the film thickness, small deviations in the alignment of the capillaries and, consequently,

Table 2. Induction Times in Different Aqueous Solutions, Total Organic Carbon (TOC), and Surface Pressure (π) of the Synthetic Produced Waters from Crude Oils A and H

	induction time (s)				
	ultrapure water	synthetic brine	synthetic produced water	TOC (ppm)	π (mN/m)
crude oil A	no rupture	8.00 ± 3.04	10.44 ± 1.55	110 ± 2	8.96 ± 0.06
crude oil H	no rupture	6.34 ± 2.21	7.86 ± 1.34	34 ± 2	5.95 ± 0.06

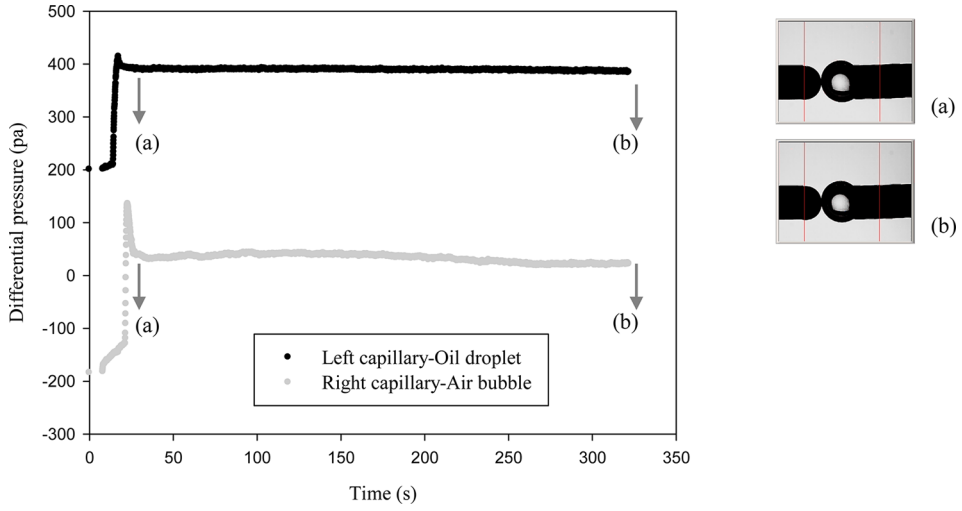

Figure 3. Differential pressure curves for a drop of crude oil H and an air bubble in ultrapure water: (a) first contact (i.e., gap = 0) between the droplet and bubble, while (b) more than 3 min of measurement time.

the bubble and drop formed at the end of capillaries, and slight differences in drop shape because of differences in viscosity.

3.1.2. Influence of Water Composition. Induction time measurements were carried out in three different water phases for crude oils A and H. The results are listed in Table 2, and it was seen that the thin film separating the drop and bubble did not rupture for any of the crude oils in ultrapure water. This is further illustrated in Figure 3, where the differential pressures for both the drop and bubble were stable for the duration of the measurements (see Video b of the Supporting Information). The very stable films were attributed to strong electrostatic repulsive forces in ultrapure water. It is well-known that the surface of air bubbles acquires negative charges in water and also in the absence of surface-active compounds.[16,24,25] Moreover, it has been demonstrated that nonpolar model oils acquire negative charges in aqueous solution without any surfactants or other additives present. The origin of charges was attributed to preferential adsorption of hydroxyl ions at the oil/water interface.[26−29] Recently, it was also reported that hydroxyl ions might contribute to highly negative charges on crude oil−water interfaces as well.[30] Consequently, electrostatic repulsion between the negatively charged oil drop and air bubble because of extended electrical double layers inhibited the film drainage and rupture in ultrapure water.

The high ionic strength in the synthetic brine solutions effectively compressed the electrical double layers and removed the double-layer repulsion between the drop and bubble. This favored drainage and rupture of the thin film within seconds. Accumulation of surface-active components at the oil−water interface is also facilitated at high ionic strength.[31] For crude oil A, for example, the oil−water interfacial tension decreased from 17.5 mN/m in the pure water to 10.1 mN/m in the brine. Because this decrease in interfacial tension was not associated with an increased induction time, it is clear that the effect of the presence of salt ions on the induction time is dominated by the double-layer compression rather than increased amounts of interfacially active compounds at the oil droplet interface.

Previously, we have demonstrated that organic crude oil compounds dissolved in the water phase adsorb onto water−air interfaces within milliseconds.[32,33] During the measurements in pure water or brine, components from the crude oil can partition into the water phase. However, the oil−water ratio is very low, and most likely, the aqueous phase does not become saturated with water-soluble components during the time frame of the experiments. To study the influence of dissolved organic components in more detail, synthetic produced water samples were prepared by mixing crude oil and water (50:50, vol %) for 24 h.[32] As shown in Table 2, both the amount of water-soluble organics (i.e., TOC) and the surface pressure of the air bubbles (after about 10 s) were highest for the produced water resulting from crude oil A. Also, the induction time was higher in the synthetic produced water from crude oil A. In both cases, the induction times were slightly higher in synthetic produced water than in the brine solution. This means that the amount of dissolved components in the aqueous phase influenced the induction times. A considerably shorter characteristic time of the adsorption of dissolved crude oil hydrocarbons (within milliseconds) compared to thin film drainage time (within seconds) ensured accumulation of dissolved components at the bubble surfaces. This can then increase the potential energy barrier that must be overcome before rupture of the thin aqueous film occurs. Furthermore, the dissolved hydrocarbons contribute to increased viscosity of the aqueous phase, which could also affect the thin film stability. The viscosity (at 25 °C) was measured to 0.89 and 1.14 mPa s for the ultrapure water and synthetic produced water of crude oil A, respectively.

3.2. Coverage Time Measurements. Subsequent to rupture of the thin aqueous film, spreading of the crude oil droplets over the air bubbles was seen for all of the investigated systems. This confirmed that the air−brine interfacial tension was high enough to ensure positive spreading coefficients. However, the time required for the oil drop to spread and completely cover the bubble varied between the crude oils. This time is referred to as the coverage time for the samples and was determined using the differential pressures recorded across the oil drop interfaces, as illustrated in Figure 4 for crude oils A, B, and C (see Video c of the Supporting Information). The first rapid pressure drops correspond to rupture of the thin films, while the subsequent gradual decrease in the pressures (indicated by circles and arrows in the figure) toward stable values was assigned to the spreading of oil over the bubbles. All of the indicated times for pressure changes were also verified by visual inspection of the corresponding videos (see the Supporting Information). The coverage time (i.e., $t_e - t_d$) for

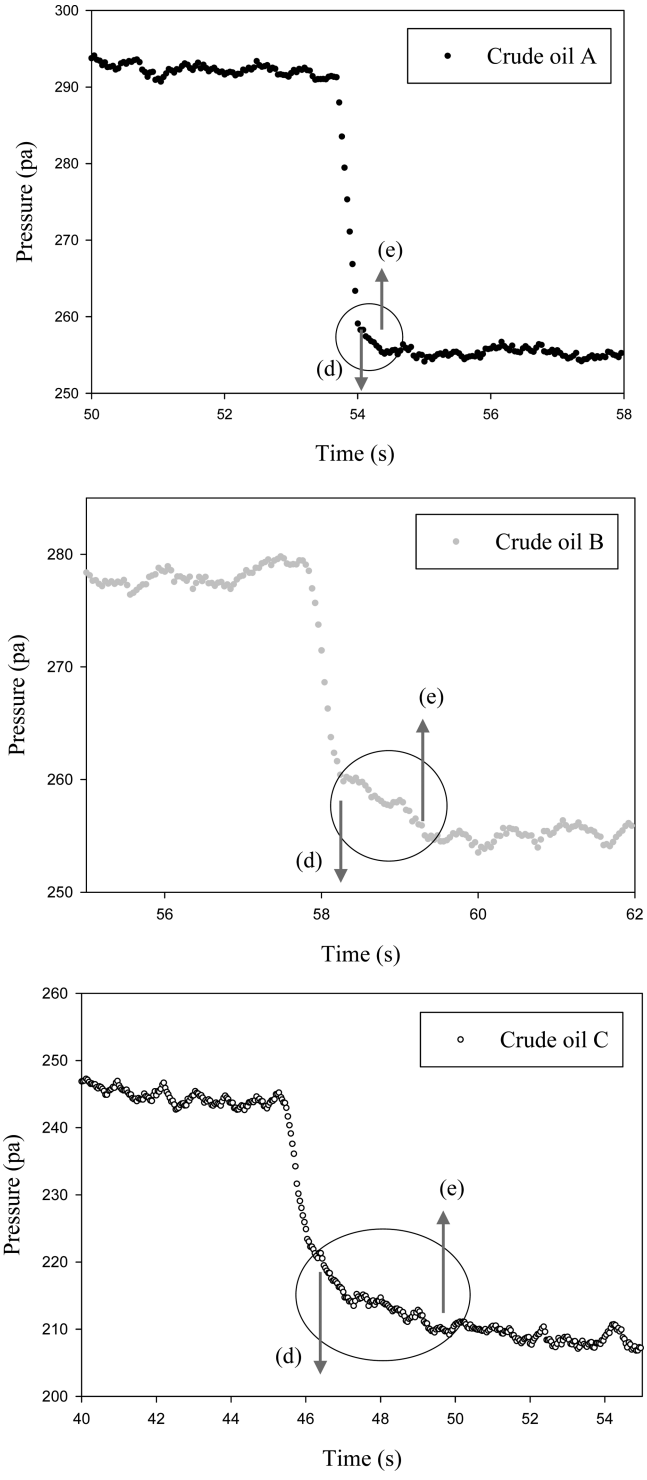

Figure 4. Dynamic differential pressure across the oil droplet interface for crude oils A, B, and C: (d) thin film ruptured and oil starts to spread onto the air bubble surface, and (e) oil covers the surface of the air bubble.

the different crude oils is presented in Table 1. The coverage time varies from below 1 s for crude oil A to about 5 s for crude oils C and G. Figure 5 shows the coverage time as a function of viscosity of crude oils, and it is clear that the coverage time tends to increase as the viscosity of the crude oil becomes higher. In most cases, the coverage time was shorter than the induction time, but the opposite was the case for the two most

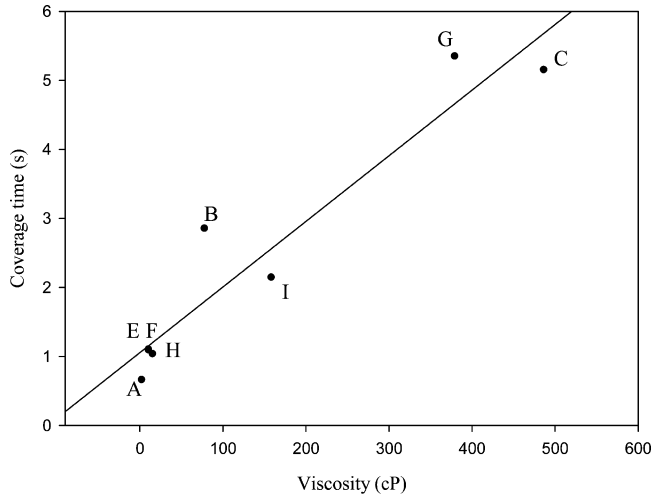

Figure 5. Average coverage time versus viscosity of crude oils.

viscous oils (crude oils C and G). Notably, crude oil A, the lightest oil with a short coverage time, exhibited a long induction time. Crude oil C, which had a short induction time, had a significantly longer coverage time. It can be concluded that the induction times were mainly influenced by interfacial properties (both crude oil droplets and air bubbles), while the manner in which the oil droplets spread and the extent that they deformed during spreading over the air bubbles depended upon the relative strength of interfacial tension and viscous forces. This can be explained by the classical capillary number $Ca = \mu U/\gamma$, which describes the strength of the viscous effect to the interfacial effect [μ is the viscosity of the spreading fluid (oil); U is the spreading velocity; and γ is the interfacial tension].[34,35] Moreover, theoretical studies on spreading kinetics in both complete and partially wetting regimes have shown that a high viscosity ratio [i.e., viscosity of the external phase (water) to the viscosity of the spreading fluid (oil)] leads to faster spreading.[36] This is in good agreement with our findings. Similar observations were also reported by others.[5]

3.3. Possible Implications for Oil Removal during Gas Flotation. The efficiency of oil drop removal in a flotation process involving dispersed bubbles will depend upon collision frequency between bubbles and drops, attachment efficiency, and stability of the bubble−drop agglomerates.[6,37−40] The collision frequency is determined by properties, such as water flow, gravitational and inertial forces, and relative velocity of the dispersed phases.[39] The attachment efficiency is related to the drainage and rupture of the thin liquid film, and the efficiency will increase with a decreased induction time.[39,40] Furthermore, it seems reasonable to anticipate that the coverage time could influence the stability of bubble−drop aggregates. At short coverage times, stable oil films surrounding the bubbles would form quickly, resulting in stable bubble−drop agglomerates that can easily be flotated. The longer the coverage time, however, the easier the detachment of oil drops from bubbles could be expected in the dynamic conditions in a flotation process, and the oil removal efficiency would be lowered. Consequently, it seems reasonable that both induction time and coverage time could be important for the detailed understanding of the flotation mechanisms. It is also noteworthy to mention that both the rupture of the thin film and the spreading of oil droplets over air bubbles will occur faster in the dynamic conditions of turbulent flow in a real process. However, we

speculate that the relative differences and trends could be similar to those observed in this study. Flotation tests are currently being carried out to investigate this further.

■ ASSOCIATED CONTENT

Supporting Information

Ionic composition of the brine (Table S1) and recorded videos of experiments showing the procedure for measuring induction time (Figure 2; Video a), stable thin film between the oil droplet and air bubble in ultrapure distilled water (Figure 3; Video b), and slow spreading of crude oil C (Figure 4; Video c). This material is available free of charge via the Internet at http://pubs.acs.org.

■ AUTHOR INFORMATION

Corresponding Author

*Telephone: +47-73-59-41-35. E-mail: gisle.oye@chemeng.ntnu.no.

Notes

The authors declare no competing financial interest.

■ ACKNOWLEDGMENTS

The authors are grateful to the industrial sponsors (ConocoPhillips Skandinavia, ENI Norge, Schlumberger Norge Division M-I EPCON, Statoil Petroleum, and Total E&P Norge) of the joint industrial program "Produced Water Management: Fundamental Understanding of the Fluids" for financial support.

■ REFERENCES

(1) Norsk olje og gass website; http://reports.norskoljeoggass.no/en/stats/.

(2) Moosai, R.; Dawe, R. A. Gas attachment of oil droplets for gas flotation for oily wastewater cleanup. *Sep. Purif. Technol.* **2003**, *33* (3), 303−314.

(3) Rubio, J.; Souza, M. L.; Smith, R. W. Overview of flotation as a wastewater treatment technique. *Miner. Eng.* **2002**, *15* (3), 139−155.

(4) Melo, M. V.; Sant'Anna, G. L.; Massarani, G. Flotation techniques for oily water treatment. *Environ. Technol.* **2003**, *24* (7), 867−876.

(5) Grattoni, C.; Moosai, R.; Dawe, R. A. Photographic observations showing spreading and non-spreading of oil on gas bubbles of relevance to gas flotation for oily wastewater cleanup. *Colloids Surf., A* **2003**, *214* (1−3), 151−155.

(6) Oliveira, R. C. G.; Gonzalez, G.; Oliveira, J. F. Interfacial studies on dissolved gas flotation of oil droplets for water purification. *Colloids Surf., A* **1999**, *154* (1−2), 127−135.

(7) Ata, S.; Pugh, R. J.; Jameson, G. J. The influence of interfacial ageing and temperature on the coalescence of oil droplets in water. *Colloids Surf., A* **2011**, *374* (1−3), 96−101.

(8) *Bubble and Drop Interfaces*; Miller, R., Liggieri, L., Eds.; CRC Press: Boca Raton, FL, 2010.

(9) Ata, S. Coalescence of bubbles covered by particles. *Langmuir* **2008**, *24* (12), 6085−6091.

(10) Chan, D. Y. C.; Klaseboer, E.; Manica, R. Film drainage and coalescence between deformable drops and bubbles. *Soft Matter* **2011**, *7* (6), 2235−2264.

(11) Kumar, M. K.; Mitra, T.; Ghosh, P. Adsorption of ionic surfactants at liquid−liquid interfaces in the presence of salt: Application in binary coalescence of drops. *Ind. Eng. Chem. Res.* **2006**, *45* (21), 7135−7143.

(12) Giribabu, K.; Ghosh, P. Adsorption of nonionic surfactants at fluid−fluid interfaces: Importance in the coalescence of bubbles and drops. *Chem. Eng. Sci.* **2007**, *62* (11), 3057−3067.

(13) Kumar, M. K.; Ghosh, P. Coalescence of air bubbles in aqueous solutions of ionic surfactants in presence of inorganic salt. *Chem. Eng. Res. Des.* **2006**, *84* (8), 703−710.

(14) Bommaganti, P. K.; Kumar, M. V.; Ghosh, P. Effects of binding of counterions on adsorption and coalescence. *Chem. Eng. Res. Des.* **2009**, *87* (5), 728−738.

(15) Duerr-Auster, N.; Gunde, R.; Mäder, R.; Windhab, E. J. Binary coalescence of gas bubbles in the presence of a non-ionic surfactant. *J. Colloid Interface Sci.* **2009**, *333* (2), 579−584.

(16) Samanta, S.; Ghosh, P. Coalescence of air bubbles in aqueous solutions of alcohols and nonionic surfactants. *Chem. Eng. Sci.* **2011**, *66* (20), 4824−4837.

(17) Nikolov, A. D.; Randie, M.; Shetty, C. S.; Wasan, D. T. Chemical demulsification of oil-in-water emulsion using air-flotation: The importance of film thickness stability. *Chem. Eng. Commun.* **1996**, *152*−*153* (1), 337−350.

(18) Gawel, B.; Eftekhardadkhah, M.; Øye, G. An elemental composition and FT-IR spectroscopy analysis of crude oils and their fractions, **2013**, Submitted to Energy Fuels.

(19) Won, J. Y.; Krägel, J.; Makievski, A. V.; Javadi, A.; Gochev, G.; Loglio, G.; Pandolfini, P.; Leser, M. E.; Gehin-Delval, C.; Miller, R. Drop and bubble micro manipulator (DBMM)—A unique tool for mimicking processes in foams and emulsions. *Colloids Surf., A* **2013**, DOI: 10.1016/j.colsurfa.2013.04.027.

(20) Shi, Q.; Hou, D.; Chung, K. H.; Xu, C.; Zhao, S.; Zhang, Y. Characterization of heteroatom compounds in a crude oil and its saturates, aromatics, resins, and asphaltenes (SARA) and non-basic nitrogen fractions analyzed by negative-ion electrospray ionization Fourier transform ion cyclotron resonance mass spectrometry. *Energy Fuels* **2010**, *24* (4), 2545−2553.

(21) Cho, Y.; Na, J.-G.; Nho, N.-S.; Kim, S.; Kim, S. Application of saturates, aromatics, resins, and asphaltenes crude oil fractionation for detailed chemical characterization of heavy crude oils by Fourier transform ion cyclotron resonance mass spectrometry equipped with atmospheric pressure photoionization. *Energy Fuels* **2012**, *26* (5), 2558−2565.

(22) Valkovska, D. S.; Danov, K. D. Influence of ionic surfactants on the drainage velocity of thin liquid films. *J. Colloid Interface Sci.* **2001**, *241* (2), 400−412.

(23) Del Castillo, L. A.; Ohnishi, S.; Horn, R. G. Inhibition of bubble coalescence: Effects of salt concentration and speed of approach. *J. Colloid Interface Sci.* **2011**, *356* (1), 316−324.

(24) Elmahdy, A. M.; Mirnezami, M.; Finch, J. A. Zeta potential of air bubbles in presence of frothers. *Int. J. Miner. Process.* **2008**, *89* (1−4), 40−43.

(25) Qu, X.; Wang, L.; Karakashev, S. I.; Nguyen, A. V. Anomalous thickness variation of the foam films stabilized by weak non-ionic surfactants. *J. Colloid Interface Sci.* **2009**, *337* (2), 538−547.

(26) Boyson, T. K.; Pashley, R. M. A study of oil droplet coalescence. *J. Colloid Interface Sci.* **2007**, *316* (1), 59−65.

(27) Marinova, K. G.; Alargova, R. G.; Denkov, N. D.; Velev, O. D.; Petsev, D. N.; Ivanov, I. B.; Borwankar, R. P. Charging of oil−water interfaces due to spontaneous adsorption of hydroxyl ions. *Langmuir* **1996**, *12* (8), 2045−2051.

(28) Beattie, J. K.; Djerdjev, A. M. The pristine oil/water interface: Surfactant-free hydroxide-charged emulsions. *Angew. Chem., Int. Ed.* **2004**, *43* (27), 3568−3571.

(29) Beattie, J. K.; Djerdjev, A. M.; Franks, G. V.; Warr, G. G. Dipolar anions are not preferentially attracted to the oil/water interface. *J. Phys. Chem. B* **2005**, *109* (33), 15675−15676.

(30) Farooq, U.; Simon, S.; Tweheyo, M. T.; Sjöblom, J.; Øye, G. Electrophoretic measurements of crude oil fractions dispersed in aqueous solutions of different ionic compositions—Evaluation of the interfacial charging mechanisms. *J. Dispersion Sci. Technol.* **2013**, *34* (10), 1376−1381.

(31) Farooq, U.; Simon, S.; Tweheyo, M. T.; Øye, G.; Sjöblom, J. Interfacial tension measurements between oil fractions of a crude oil and aqueous solutions with different ionic composition and pH. *J. Dispersion Sci. Technol.* **2013**, *34* (5), 701−708.

(32) Eftekhardadkhah, M.; Øye, G. Dynamic adsorption kinetics of organic compounds dissolved synthetic produced water at air bubbles: The influence of the ionic composition of aqueous solutions. *Energy Fuels* **2013**, *27* (9), 5128−5134.
(33) Eftekhardadkhah, M.; Reynders, P.; Øye, G. Dynamic adsorption of water soluble crude oil components at air bubbles. *Chem. Eng. Sci.* **2013**, *101*, 359−365.
(34) Voinov, O. V. Spreading of a drop of viscous liquid over a surface under the action of capillary forces. *J. Appl. Math. Mech.* **1995**, *59* (5), 735−743.
(35) Liang, Z.-P.; Wang, X.-D.; Duan, Y.-Y.; Min, Q. Energy-based model for capillary spreading of power-law liquids on a horizontal plane. *Colloids Surf., A* **2012**, *403*, 155−163.
(36) Foister, R. T. The kinetics of displacement wetting in liquid/liquid/solid systems. *J. Colloid Interface Sci.* **1990**, *136* (1), 266−282.
(37) Nguyen, A. V.; Ralston, J.; Schulze, H. J. On modelling of bubble−particle attachment probability in flotation. *Int. J. Miner. Process.* **1998**, *53* (4), 225−249.
(38) Ralston, J.; Fornasiero, D.; Hayes, R. Bubble−particle attachment and detachment in flotation. *Int. J. Miner. Process.* **1999**, *56* (1−4), 133−164.
(39) Min, M. A.; Nguyen, A. V. An exponential decay relationship between micro-flotation rate and back-calculated induction time for potential flow and mobile bubble surface. *Miner. Eng.* **2013**, *40*, 67−80.
(40) *Colloidal Science of Flotation*; Nguyen, A. V., Schulze, H. J., Eds.; Marcel Dekker: New York, 2004.